Measurements of blue shifts due to collisionless absorption in harmonic generation from subpicosecond laser-produced plasmas

A. Ishizawa,[1,*] R. A. Ganeev,[1,2] T. Kanai,[1] H. Kuroda,[1] and T. Ozaki[1,3]
[1]*Institute for Solid State Physics, University of Tokyo, 5-1-5 Kashiwanoha, Kashiwa, Chiba 277-8581, Japan*
[2]*NPO Akadempribor, Academy of Sciences of Uzbekistan, Tashkent 700143, Uzbekistan*
[3]*NTT Basic Research Laboratories, NTT Corporation, 3-1, Morinosato Wakamiya, Atsugi-shi, Kanagawa pref. 243-0198, Japan*
(Received 30 July 2001; revised manuscript received 25 March 2002; published 28 August 2002)

Harmonic generation from solid surface plasmas is studied using a subpicosecond Nd:glass laser system. For a 45° angle of incidence, the speculars up to the fifth harmonics are blue shifted when the laser intensity exceeds 2×10^{16} W cm^{-2}. The second harmonic is blueshifted by ~16 Å, and the fifth harmonic is blue shifted by ~51 Å for *p* polarization at the intensity of 1×10^{17} W cm^{-2}. We observed the blue shift of the fifth harmonics and found that the magnitude of blue shift is higher compared with that for the second harmonics. The blue shift is interpreted as a collisionless absorption due to the anomalous skin effect. It is also found that the divergence of harmonics preserves a smaller divergence when using a shorter pulse length for the driving laser.

DOI: 10.1103/PhysRevE.66.026414 PACS number(s): 52.50.Jm, 42.65.Ky, 52.35.Mw

I. INTRODUCTION

The recent availability of compact, high-intensity subpicosecond lasers with chirped pulse amplification (CPA) [1] has opened the new field of study of laser-matter interactions with solid targets. Thus, using a compact high-intensity laser system, it is now possible to study laser-matter interaction for the fast ignition scheme for inertial confinement ignition [2], harmonic generation from solid surface [3,4], and ultrashort x-ray generation [5], etc. The study of laser-plasma interactions have been performed for several decades. As is well known at low intensity and long pulse length, the dominant absorption mechanism is inverse bremsstrahlung and classical resonance absorption [6]. With the recent advent of subpicosecond pulse length and high-intensity lasers, short density gradient scale length $L/\lambda \ll 1$, where λ is the laser wavelength, can be formed because there is no time for the free electron to expand into the vacuum region. We define the electron density gradient scale length L as the inverse of the logarithmic derivative $[(1/n_e)(dn_e/dx)]^{-1}$, where n_e is the upper shelf density [7]. It becomes important to investigate several additional absorption mechanisms for short pulse length and high-intensity laser pulses interacting with overdense plasmas. At high laser intensities above 10^{16} W cm^{-2}, the electron temperature is more than 1 keV and the main laser absorption is related to collisionless absorption. Collisionless absorption mechanisms include vacuum heating, $\mathbf{J}\times\mathbf{B}$ heating, sheath inverse bremsstrahlung, and the anomalous skin effect [8,9]. Recently, Hansen *et al.* reported for the first time that the second harmonic was blue shifted when the laser intensity exceeded 5×10^{16} W cm^{-2} and this effect was also observed in particle-in-cell (PIC) simulations [10]. For an angle of incidence of 55°, the second harmonic emission was not blue shifted, and it was observed that the second harmonic signal for *p* polarization was ten times higher than for *s* polarization. This result shows the resonance absorption is dominant at this angle of incidence. On the other hand, for an angle of incidence of 17.5°, the specular second harmonic was blue shifted by ~60 Å when the laser intensity exceeded 1.5×10^{17} W cm^{-2}. The simulation result showed the electron temperature at the skin depth was 800 eV and had no collision. The electrons can be driven into the target a distance greater than the skin depth, and collisionless absorption dominates the absorption process. If the frequency of the oscillation of the electrons changes with its amplitude, the electronmagnetic field will drive the oscillation out of resonance. It results in changing the frequency of the harmonic radiation. There are, however, some questions as to how much the other harmonic order is blue shifted and whether the harmonics is blue shifted at an angle of incidence of 45° between 17.5° and 55°. It is, therefore, timely to study the absorption mechanism in subpicosecond high-intensity laser-plasma interaction. The purpose of this paper is to show how the other harmonic order is blue shifted and whether at the angle of incidence of 45° the harmonics is blue shifted or not.

In this paper, we present blue shifts of up to 20 Å in the second harmonic and 50 Å in the fifth harmonic by the irradiation of a solid target with a 500-fs laser pulse for *p* polarization, an incident angle of 45°, and laser intensities above 3×10^{16} W cm^{-2}. We observed the blue shift of the fifth harmonics and found that the magnitude of blue shift is higher compared with that for the second harmonics. We carry out more detailed model calculations of the electron temperature in our experimental condition using a one-dimensional (1D) hydrodynamic code HYADES [11]. We find that the blue shift in our experiment can be well explained from the absorption mechanism due to the anomalous skin effect. The divergence and intensity of the harmonics using 500 fs pulse length for the driving laser is compared with using 2.2 ps pulse length. It is found that to keep the harmonics collimated even when the intensity of the driving

*Email address: ishizawa@issp.u-tokyo.ac.jp

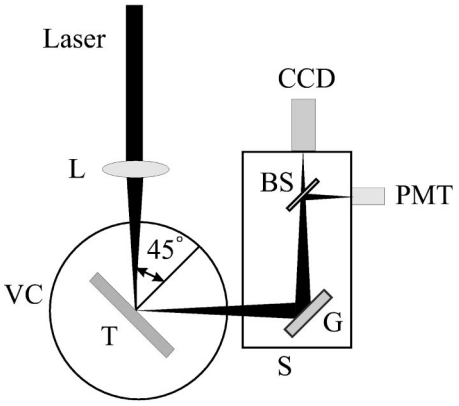

FIG. 1. Experimental arrangement. *L*, achromatic lens; VC, vacuum chamber; *T*, aluminum deposited target; *S*, spectrograph; G, grating; BS, beam splitter (CaF_2).

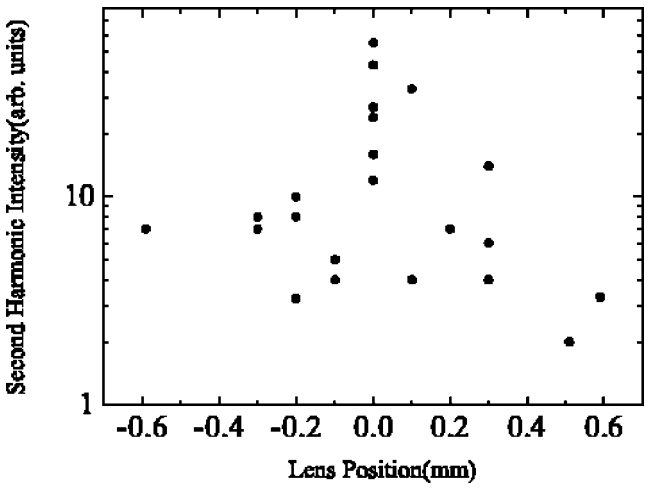

FIG. 2. The second harmonic intensities as a function of the lens position. We can find the optimum position of the lens by measuring the second harmonic signal using the CCD camera in the experiment.

laser is increased, driving lasers with shorter pulse lengths should be used.

II. EXPERIMENTAL SETUP

The schematic diagram of the experimental arrangement is shown in Fig. 1. The experiments were carried out at the Institute for Solid State Physics in the University of Tokyo with a CPA Nd:glass laser system [12] operating at a wavelength of around 1060 nm and at a repetition rate of one shot for every 5 min. The contrast ratio of each pulse is better than 10^{-6}. The laser delivered 100 mJ energy in a 500-fs pulse and produced a peak intensity on the target of 2×10^{17} W cm^{-2} at a laser focus of 12 μm diameter placed in the vacuum chamber. The laser pulse is focused onto the surface of a solid target with a 10 cm focal length achromatic lens at an incidence angle of 45° relative to the target normal with either *s* or *p* polarization selected using a $\lambda/2$ wave plate. We can find the optimum position of the lens by measuring the second harmonic signal using a charge-coupled device (CCD) camera. The experimental result is shown in Fig. 2. The target is a 0.1-μm layer of aluminum deposited on a glass substrate. The target is moved to ensure that the laser interacts with a fresh surface of the target at each shot. Harmonics generated from the plasma surface in the specular direction are spectrally dispersed by a spectrometer (Acton Model VM-504). The spectrometer has a wavelength accuracy and resolution of ±0.2 nm at 500 nm with a 1200-g/mm grating. The CaF_2 plate is put after the light goes to the grating, and then the light is divided. Harmonics can be simultaneously detected using both a CCD camera (Hamamatsu C4880-21) and a fast rise time photomultiplier (Hamamatsu R2496, 0.7 ns rise time). The temporal profile of the output signal of the photomultiplier is measured with a 1.5 GHz bandwidth oscilloscope (Lecroy 9362).

III. RESULTS AND DISCUSSION

A. Wavelength shift

It is very important that we investigate the spectral and spatial analysis of harmonics to understand the information on the critical density surface and overdense plasmas surface when the incident laser interacts with the plasma. As is well known, the resonance absorption process is dominant when incident laser intensity is under 1×10^{16} W cm^{-2}. If the resonance absorption process is dominant, harmonic frequency is not shifted except for Doppler shifts of reflected light arising from plasma expansion driven by the heated electrons [13,14]. We can measure the Doppler shift in the reflected 1060 nm. The fundamental is blue shifted by ~6 Å corresponding to an expansion velocity $c_s/c\approx6\times10^{-4}$. Figure 3 summarizes the experimental results of the second harmonic. The results are inconsistent with the resonant absorption: (1) the second harmonic light is blue shifted by ~16 Å [see Figs. 3(a) and 3(b)] for *p* polarization and the second harmonic signal for *p* polarization is about eight times higher than that for *s* polarization at the fundamental laser intensity of $\sim10^{17}$ W cm^{-2}. (2) The dependence of the wavelength shift on the incident laser intensity is shown in Fig. 3(c). The peak frequency of the second harmonic emission is blue shifted for $I_L\geqslant2\times10^{16}$ W cm^{-2}, where I_L is the incidence laser intensity. It is found that the increase of this shift width with an increase in the laser intensity is small in comparison with the experimental results by Hansen *et al.* [10]. Unfortunately, we cannot detect the shift below $I_L\leqslant1\times10^{16}$ W cm^{-2} by using this system. We cannot correctly measure the peak frequency of the third and fourth harmonic emission in this system because the signal-to-noise ratio is poor. There are two reasons. (1) The diffraction grating efficiency is low for the above two harmonic wavelengths, and (2) there are line emissions from aluminum ions in the vicinity of these harmonics. Figure 4 shows the experimental results of the fifth harmonic. The fifth harmonic light is blue shifted by ~51 Å [see Figs. 4(a) and 4(b)] for *p* polarization at the intensity of $I_L\geqslant1\times10^{17}$ W cm^{-2}. This shift is much larger in magnitude than the Doppler shift seen in the spectrum of the fundamental. Therefore, these results cannot be explained by the hydrodynamic motion of plasma.

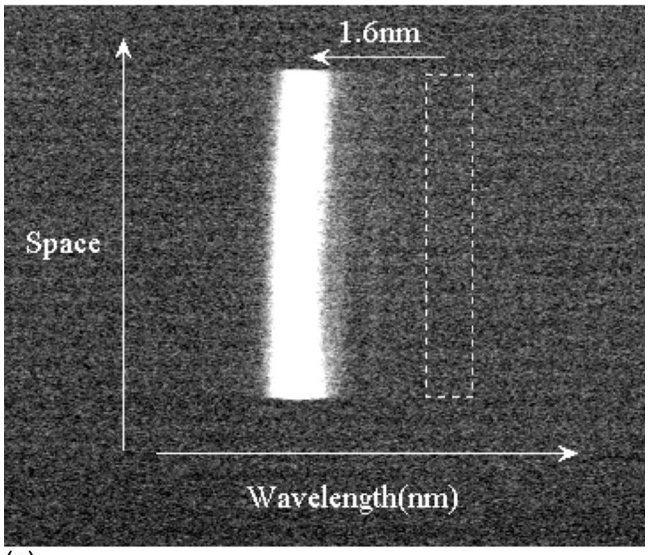

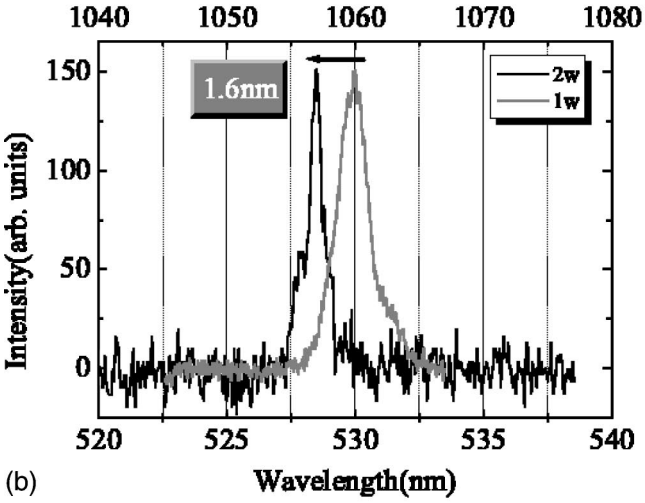

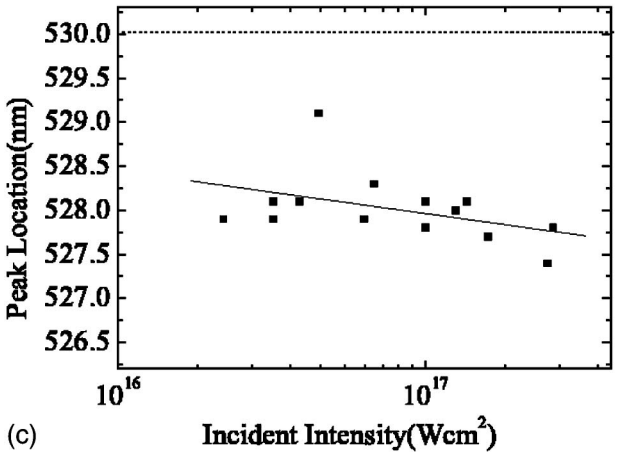

FIG. 3. Summary of the second harmonic in the experiments. (a) The picture of the second harmonic and the dashed line is the position of twice frequency of the fundamental laser. (b) The second harmonic spectrum (black line) and the incident laser spectrum (gray line) at the laser intensity of 1.5×10^{17} W cm^{-2}. (c) Location of the second harmonic peak as a function of incident intensity.

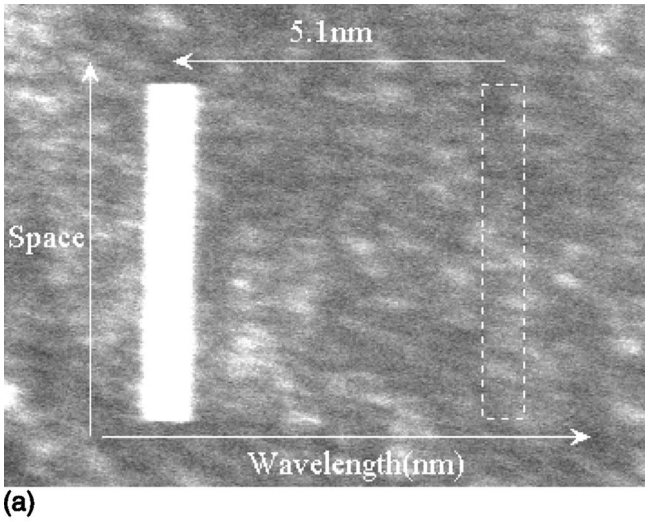

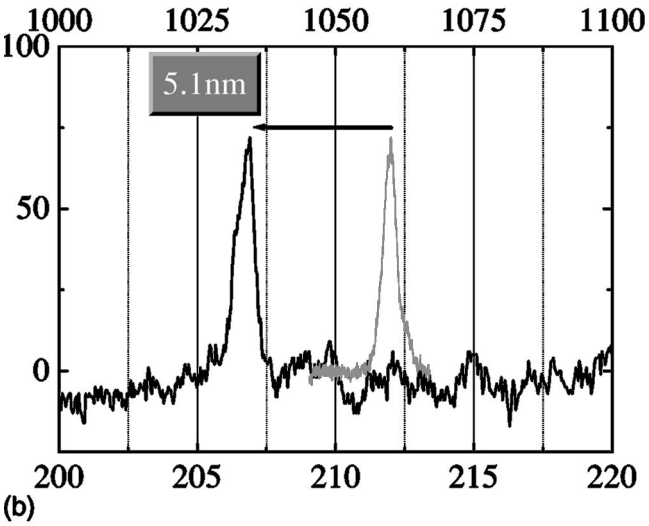

FIG. 4. Summary of the fifth harmonic in the experiments. (a) The picture of the fifth harmonic and the dashed line is the position of fifth frequency of the fundamental laser. (b) The fifth harmonic spectrum (black line) and the incident laser spectrum (gray line) at the laser intensity of 1.6×10^{17} W cm^{-2}.

With increasing laser intensity and electron temperature, the role of collisions decreases and collisionless mechanisms of absorption become dominant [8,9]. The experimental and PIC simulation results by Hansen *et al.* [10] show that the second harmonic due to collisionless absorption occurs when the laser intensity exceeds 5×10^{16} W cm^{-2}. The calculation results by Rozmus *et al.* [8] show that at low temperature ($T_e<300$ eV), the collision absorption mechanism is dominant, and at higher temperature ($T_e>800$ eV), the collisionless absorption mechanism due to the anomalous skin effect becomes dominant. The electronic temperature profile in our experiment condition was calculated using a 1D hydrodynamic code HYADES [11]. The reliability of the 1D HYADES code is confirmed in Ref. [16]. We observe the transverse intensity profile of the transmitted 2.2-ps, *p* polarized longitudinal laser beam using a CCD camera after interaction with the preplasma. Numerical simulations are performed on the

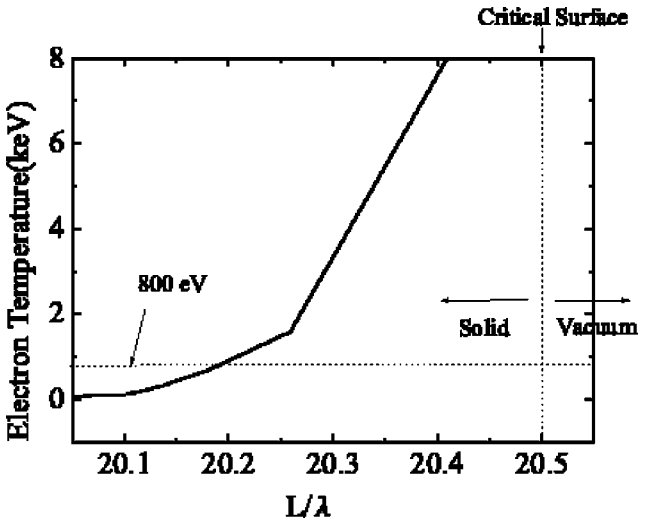

FIG. 5. The electron temperature for our experimental condition, obtained from 1D HYADES code at the same time of the peak of laser pulse at the incident laser intensity of 1×10^{17} W cm^{-2}.

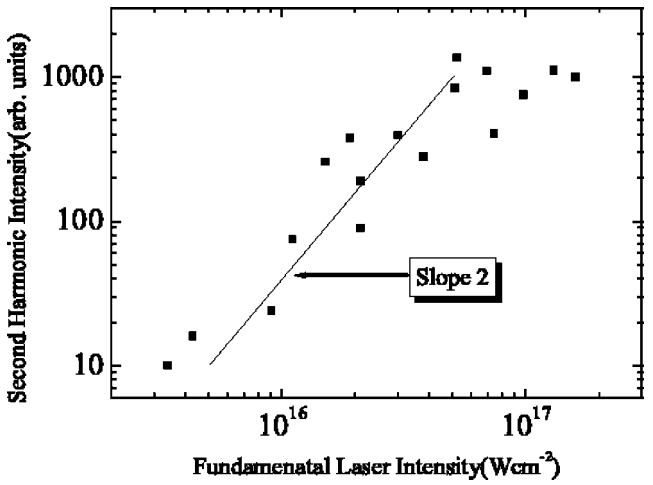

FIG. 6. The second harmonic intensity as a function of incident intensity in the experiment. The black line represents the power law of the form $I_{2\omega}\sim I_{\omega}^{2}$.

model of experimental observation, using a 1D HYADES code and a paraxial approximation ray tracing code. Using the various outputs from these codes, we then calculate the intensity profile of the transmitted laser beam and compare the results with our experimental observations. The overall profile is excellently reproduced. Both inverse bremsstrahlung and collisionless absorption are included. These are calculated from the average of $\mathbf{E}\cdot\mathbf{J}$, since $\mathbf{J}$ depends on the conductivity, which is a function of the dielectric function and thus the electron-ion collision frequency. Figure 5 shows the electron temperature profile for our experimental conditions when the main pulse laser intensity on the solid target is 1×10^{17} W cm^{-2} by using 1D HYADES code. We can see from this figure that the electron temperature in the skin depth from the critical density surface is much higher than 800 eV. The higher temperature (>800 eV) is enough to reduce the importance of collisions on the plasma behavior. The calculation results by Rozmus *et al.* [8] show that at the higher temperature (>800 eV) the absorption is almost a collisionless mechanism. Hansen *et al.* [10] have observed a blue shift in the second harmonic at the electron temperature ($T_e\sim800$ eV) in PIC simulation. Therefore, we can conclude that from our experimental and calculation results the harmonic frequency shift is due to the collisionless mechanism. We treat the skin depth in the collisionless absorption as the phase shifter. When the driving laser irradiates the solid target, the electrons' phase become the same phase of the driving laser field. Each electron in the plasma passes the skin depth in the collisionless absorption condition and shifts the phase in the skin depth. Then, each electron is reversed in direction and returns to the plasma. It is considered that the electron pumps up to the upper level at virtual time in the multiphoton absorption process. Therefore, the electron's phase is accumulated and locked by this process. The phase-locked electrons couple in each resonace layer and then high order harmonics are generated. In this experiment, the magnitude of the blue shift of the fifth harmonics is 2.2–3.1 times higher compared with that for the second harmonics. It is considered that the magnitude of blue shift is in proportion to the phase. Hansen *et al.* also reported that if the phase change is averaged over a cycle, weighed by amplitude, there would be a net increase in frequency. The phase between the second and fifth harmonics should be different. It is possible to attribute the difference in the wavelength shift between the orders of harmonics in our experimental results to the phase shift accumulation or phase shift rotation at a certain cycle. In an upcoming paper, we will report a more detailed analysis of the experimental data of other order harmonics.

B. Divergence and efficiency of the harmonics

In our previous work, we have measured the efficiency and the divergence of harmonics by using 2.2 ps pulse length for the driving laser [4,17,18]. For this section, it may be useful to look more closely at some of the more important features of harmonic generation from solid surface plasmas by comparing the 500 fs pulse length in this experiment with the 2.2 ps pulse length in our previous experiment. Up to now, we have performed systematic investigations of surface harmonic generation using 2.2 ps duration Nd:glass laser pulses, and clarifying such characteristics as conversion efficiency, spatial distribution, and polarization dependence of the driving laser. As a next step, we turn to compare harmonics generated from 500-fs and 2.2-ps driving lasers. In this section we show the harmonic yield dependence on the driving laser polarization.

The intensities of the second harmonics are measured at various driving laser intensities using the experimental setup of Fig. 1. We use a *p* polarized driving laser for this measurement. Figure 6 shows the observed relative intensity of the second harmonics as a function of driving laser intensity in the experiments. By fitting the data to a function $I_{m\omega}\propto(I_{\omega})^{n}$, where $I_{m\omega}$ is the intensity of the mth harmonic, we evaluate $n\sim2$ below the laser intensity of 5×10^{16} W cm^{-2}. The slope of this dependence is decreased to above 5×10^{16} W cm^{-2} for the second harmonics. When we used 2.2 ps pulse length for the driving laser, we evalu-

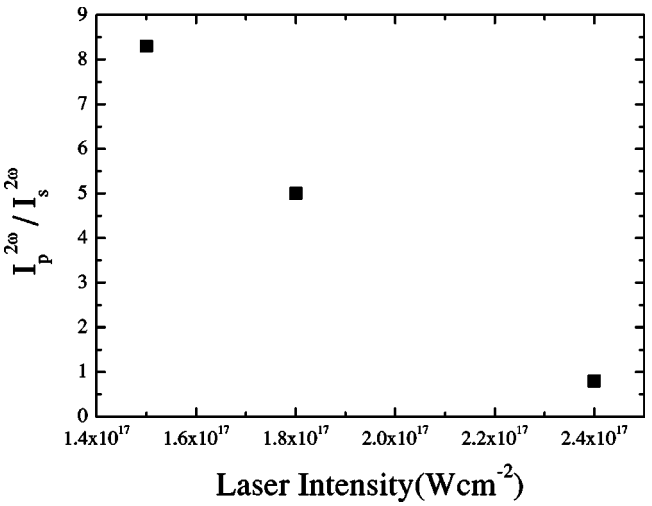

FIG. 7. The second harmonic intensity dependence on the driving laser polarization in the experiment. We find that for both harmonics, the harmonic yield dependence on the driving laser polarization decreases when the laser intensity exceeds 1×10^{17} W cm^{-2}.

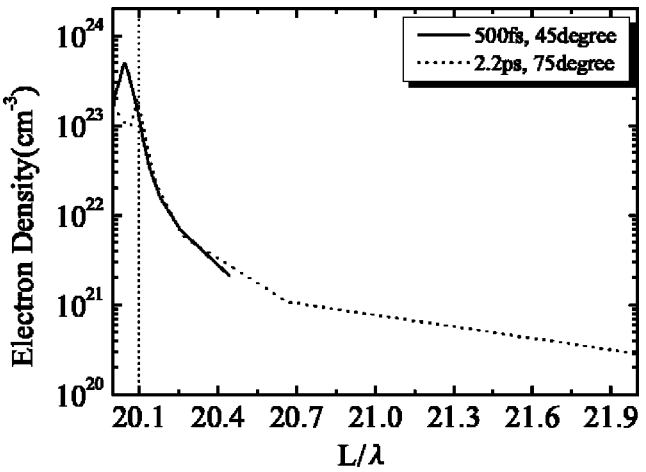

FIG. 8. The electron density distribution both for this experiment condition (500 fs pulse length and incidence angle 45°) and for the previous experimental condition (2.2 ps pulse length and incidence angle 75°), obtained from 1D HYADES code when the main pulse laser intensity is 1×10^{17} W cm^{-2}. The vertical dotted line is the Al target surface before the laser pulse irradiates the Al target.

ated $n=1\pm0.3$ [18]. The experimental results by Földes *et al.* [19] show $n=2.1\pm0.4$ using 700 fs pulse length for the driving laser. There is a possibility that a power law dependence on the laser intensity depends on the pulse length and the contrast ratio for the driving laser, the calculation results of the electron density distribution, and the efficiency of harmonics by using 500 fs and 2.2 ps pulse length.

Figure 7 shows the harmonic yield dependence on the driving laser polarization in the experiment. We find that for both harmonics, the harmonic yield dependence on the driving laser polarization decreases when the laser intensity exceeds 1×10^{17} W cm^{-2}. When the driving laser intensity is increased, the factor that causes the divergence of the harmonics to gradually increase is thought to be a Rayleigh-Taylor-like instability at the critical surface [15]. At an intensity lower than $I_L=5\times10^{16}$ W cm^{-2}, the harmonics are generated in the specular direction and the divergence is comparable to the driving laser because the plasma surface is still free from the Rayleigh-Taylor-like instability and hole boring. The plasma surface gradually leads to a rippling of the plasma surface when the driving laser intensity is increased. As a result, the divergence of the harmonics becomes wider than the divergence of the driving laser. In previous works, we measured the spatial distribution of the third to fifth harmonics using 2.2 ps and 100 ps pulse length driving lasers [17]. When we used 2.2 ps pulse length for the driving laser, the divergence of the harmonics became wider than the divergence of the driving laser at the intensity of $I_L=1\times10^{15}$ W cm^{-2}. We measured the harmonics emission when using 2.2 ps pulse length for the driving laser, and found that it is more specular than when using 100 ps pulse length. From these results, it is found that one was to keep the harmonics collimated even when the intensity of the driving laser is increased is to use driving lasers with shorter pulse lengths.

At a peak driving laser intensity of $\sim10^{17}$ W cm^{-2}, the conversion efficiencies of the second and fifth harmonics are 1×10^{-6} and 4×10^{-8}, respectively, by using 500 fs pulse length for the driving laser, and at the intensity of $\sim10^{14}$ W cm^{-2}, the efficiency of the second harmonics is 9×10^{-10} by using 300 ps pulse length. The efficiency of harmonics using 500 fs pulse length for the driving laser is consistent with the efficiency of harmonics using 2.2 ps pulse length at the same intensity.

The electronic density profile in our experimental condition was first calculated using a 1D hydrodynamic code HYADES [11]. In our group's previous work we have confirmed that Fig. 8 shows the electron density distribution by using 500 fs and 2.2 ps pulse length for the driving laser in our experimental conditions when the driving laser intensity on the solid target is 1×10^{17} W cm^{-2}. We can see from this figure that the electron density profile between 500 fs pulse length and 2.2 ps pulse length is very similar. We can calculate $L/\lambda<0.1$ by using both 500 fs and 2.2 ps pulse lengths for the driving laser when we decide n_e/n_c is 7, where n_c is the critical density at laser wavelength λ. A modest value of $n_e/n_c=7$ is adopted in this calculation, which is in between the corresponding values used in past works [20,21]. The contrast ratio of the driving laser is better than 10^{-6}. There is a possibility that a prepulse produces preplasma and it influences the electron density scale length actually. It is found from this results that the driving laser interacts with a steep density profile, and the interaction takes place in the skin layer of an overdense plasma ($n_e \gg n_c$).

The effect of the scale length is investigated using the LPIC code [22]. Figure 9 (a) shows the power spectra of the harmonics as a function of the order of harmonics for our experimental condition when the laser intensity is 1×10^{18} W cm^{-2} by using 1D LPIC code. We can see that the harmonic intensity using 500 fs pulse length and 2.2 ps pulse

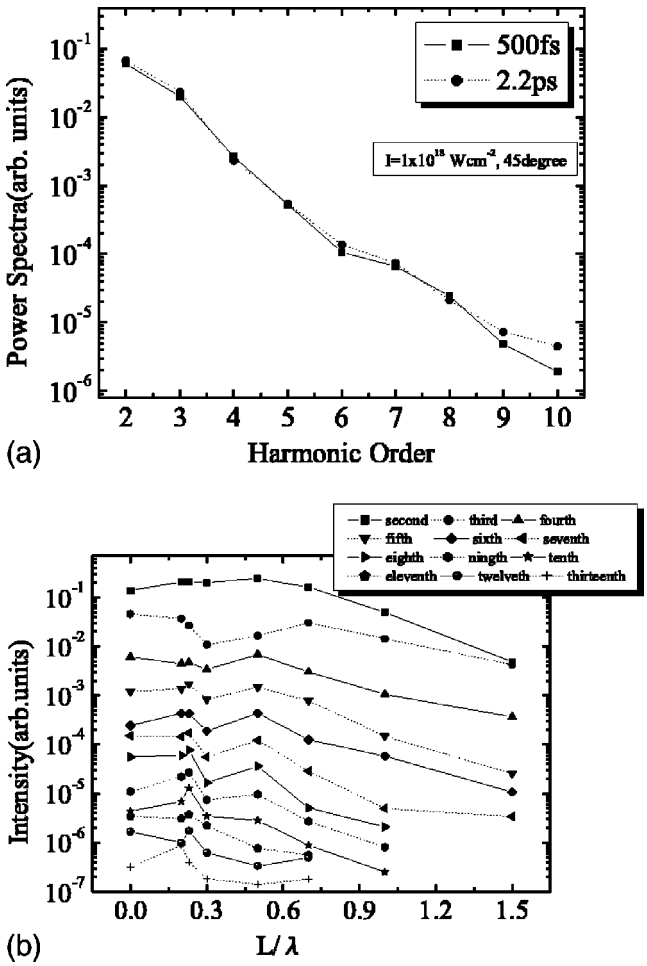

FIG. 9. (a) The harmonic intensity as a function of orders of harmonics, obtained from 1D PIC simulations at the intensity of 1×10^{18} W cm^{-2}. (b) Variation of the harmonic intensity with the density scale length L/λ of the preformed plasma.

length for the driving laser is similar. This calculation result is in good agreement with our experimental results. It is known that the harmonic efficiency depends on the laser irradiance and the density scale length [22,23]. We also calculate the harmonic intensity for our experimental condition using 1D LPIC code. Figure 9(b) shows the harmonic intensity as a function of orders of harmonics by using 1D LPIC code. It is found that the optimum scale length is $L=0.2\lambda-0.3\lambda$ in our experimental condition, and the harmonic intensity has the tendency to increase the difference between the density scale lengths when the order of harmonics is higher. We can see that the efficiency of the harmonic generation is also low when the density scale length is too large because the light amplitude driving oscillations at the critical density decrease as a result of inverse bremsstrahlung absorption, and harmonics generated from the effect of the resonant absorption is reduced. It is thought that there is a trade-off between the two harmonic generation mechanisms, which determines the optimum density scale length. We suggest we should use the double pulse lasers for producing a favorite density scale length by changing the time delay and intensity ratio between the prepulse and the main laser pulse. It is thought that the prepulse plays an important role in modulating the density scale length. In an upcoming paper, we will report a more detailed analysis of the experimental data and a more detailed theoretical description of the PIC simulation.

IV. CONCLUSION

Investigations have been performed on the harmonic generation from solid surface plasmas using the subpicosecond Nd:Glass lasers, and several interesting phenomena have been observed. The blue shift of the harmonics by collisionless process has been observed. The second harmonic is blue shifted by ~16 Å, and the fifth harmonic is blue shifted by ~51 Å for p polarization at the intensity of 1×10^{17} W cm^{-2}. It is found that the magnitude of the blue shift increases with orders of harmonic. These results are important demonstrations of the large harmonic blue shift that can provide a tool to realize a tunable coherent subpicosecond light source. It is found that the divergence of harmonics is shorter to use driving lasers with shorter pulse length. Investigations are presently underway to clarify the physics underlying these findings.

ACKNOWLEDGMENTS

The authors gratefully acknowledge the assistance by J. T. Larsen in running the HYADES code, and R. E. W. Pfund and R. Lichters in running the LPIC code. This research was partially supported by the Ministry of Education, Culture, Sports, Science and Technology Grant-in-Aid. This research was also supported by the Ministry of Education, Culture, Sports, Science and Technology, Grant-in-Aid for 11308014. R.A.G. would like to acknowledge the Ministry of Education, Culture, Sports, Science and Technology for providing financial support during his stay with the ISSP.

[1] M.D. Perry and G. Mourou, Science **264**, 917 (1994).
[2] M. Tabak *et al.*, Phys. Plasmas **1**, 1626 (1994).
[3] P.A. Norreys *et al.*, Phys. Rev. Lett. **76**, 1832 (1996).
[4] A. Ishizawa, T. Kanai, T. Ozaki, and H. Kuroda, IEEE J. Quantum Electron. **37**, 384 (2001).
[5] J.D. Kmetec *et al.*, Phys. Rev. Lett. **68**, 1527 (1992).
[6] D.F. Price *et al.*, Phys. Rev. Lett. **75**, 252 (1995).
[7] S. Bastiani *et al.*, Phys. Rev. E **56**, 7179 (1997).
[8] W. Rozmus, V.T. Tikhonchuk, and R. Cauble, Phys. Plasmas **3**, 360 (1996).
[9] S.C. Wilks and W.L. Kruer, IEEE J. Quantum Electron. **33**, 1954 (1997).
[10] C.T. Hansen, S.C. Wilks, and P.E. Young, Phys. Rev. Lett. **83**, 5019 (1999).
[11] A.M. Rubenchik, M.D. Feit, M.D. Perry, and J.T. Larsen, Appl. Surf. Sci. **129**, 193 (1998).

[12] J. Itatani *et al.*, Prog. Cryst. Growth Charact. Mater. **33**, 281 (1996).
[13] H.M. Milchberg and R.R. Freeman, Phys. Rev. A **41**, 2211 (1990).
[14] O.L. Landen and W.E. Alley, Phys. Rev. A **46**, 5089 (1992).
[15] S.C. Wilks, W.L. Kruer, M. Tabak, and A.B. Langdon, Phys. Rev. Lett. **69**, 1383 (1992).
[16] H. Kuroda, T. Ozaki, A. Ishizawa, T. Kanai, K. Yamamoto, R. Li, and J. Zhang, Proc. SPIE **4424**, 437 (2001).
[17] A. Ishizawa, T. Kanai, T. Ozaki, and H. Kuroda, IEEE J. Quantum Electron. **36**, 665 (2000).
[18] A. Ishizawa *et al.*, IEEE J. Quantum Electron. **35**, 60 (1999).
[19] I.B. Földes *et al.*, Phys. Lett. A **258**, 312 (1999).
[20] S.C. Wilks, W.L. Kruer, and W.B. Mori, IEEE Trans. Plasma Sci. **21**, 120 (1993).
[21] P. Gibbon, Phys. Rev. Lett. **76**, 50 (1996).
[22] R. Lichters and J. Meyer-ter-Vehn, Inst. Phys. Conf. Ser. **154**, 221 (1997).
[23] M. Zepf *et al.*, Phys. Rev. E **58**, R5253 (1998).